INSTITUTE OF PHYSICS PUBLISHING NANOTECHNOLOGY
Nanotechnology **14** (2003) 1029–1035 PII: S0957-4484(03)61002-0

Large-scale synthesis of arrays of high-aspect-ratio rigid vertically aligned carbon nanofibres

A V Melechko[1,2,5], T E McKnight[1,4], D K Hensley[1,4], M A Guillorn[1,3,4], A Y Borisevich[4], V I Merkulov[1], D H Lowndes[4] and M L Simpson[1,3,4]

[1] Molecular-Scale Engineering and Nanoscale Technology Research Group, Oak Ridge National Laboratory, Oak Ridge, TN 37831, USA
[2] Department of Electrical and Computer Engineering, University of Tennessee, Knoxville, TN 37996, USA
[3] Materials Science and Engineering Department, University of Tennessee, Knoxville, TN 37996, USA
[4] Condensed Matter Sciences Division, Oak Ridge National Laboratory, Oak Ridge, TN 37831, USA

E-mail: acm@ornl.gov (A V Melechko)

Received 17 March 2003, in final form 21 July 2003
Published 19 August 2003
Online at stacks.iop.org/Nano/14/1029

Abstract
We report on techniques for catalytic synthesis of rigid, high-aspect-ratio, vertically aligned carbon nanofibres by dc plasma enhanced chemical vapour deposition that are tailored for applications that require arrays of individual fibres that feature long fibre lengths (up to 20 μm) such as scanning probe microscopy, penetrant cell and tissue probing arrays and mechanical insertion approaches for gene delivery to cell cultures. We demonstrate that the definition of catalyst nanoparticles is the critical step that enables growth of individual, long-length fibres and discuss methods for catalyst particle preparation that allow the growth of individual isolated nanofibres from catalyst dots with diameters as large as 500 nm. This development enables photolithographic definition of catalyst and therefore the inexpensive, large-scale production of such arrays.

(Some figures in this article are in colour only in the electronic version)

1. Introduction

The controlled synthesis of nanoscale structures, including carbon nanotubes (CNTs) or carbon nanofibres (CNFs), is an important enabling step in the realization of practical devices containing nanoscale components. Deterministic growth of a nanostructure implies the precise control of its location, shape, orientation, internal structure and chemical composition. Recently, it was shown that vertically aligned carbon nanofibres (VACNFs) can be synthesized highly deterministically (Ren *et al* 1998, 1999, Merkulov *et al* 2000, 2002a). This ability has allowed nanofabrication of a variety of devices for potential applications in scanning electron microscopy and electron beam lithography (Guillorn *et al* 2002b), scanning probe microscopy (Hudspeth *et al* 2002) and electrochemical probes (Guillorn *et al* 2002a, Li *et al* 2002).

VACNFs similar to those described in this paper are frequently referred to in the literature as CNTs (Teo *et al* 2003). However, there is a distinct structural difference. After Ijima's (Iijima 1991) report the term 'nanotube' is usually reserved for a structure that consists of concentric graphene cylinders, while a nanofibre is usually considered to be composed of graphitic 'funnels' and cones, also referred to as 'herringbone' (e.g. Lee *et al* 2001) and 'bamboo-like' structures. Thus, the difference between VACNFs and nanotubes is not simply the higher degree of crystallinity of nanotubes, but essentially different long-range crystalline structures. As a result, the physical and chemical properties of VACNFs are expected to be quite different from those of

[5] Author to whom any correspondence should be addressed.

nanotubes, so that clear differentiation is highly desirable. The importance of this differentiation has been stressed previously (Nolan *et al* 1998, Matthews *et al* 2002).

The type of CNF and the geometry of their arrays presented in this paper have been specifically developed and successfully utilized for parallel insertion into live cells and for the delivery of DNA attached to these nanofibres into the intracellular domain (McKnight *et al* 2003). While we have performed such DNA delivery experiments with dense and sparse forests of CNFs similar to previously described arrays (e.g. Tu *et al* 2003), so far we have only succeeded in cell membrane penetration and DNA delivery to cells using long, rigid, conical, isolated, high-aspect ratio VACNFs. Here we present the characterization of such VACNFs and describe some techniques that are necessary and unique for their synthesis and that have not been reported before. Details of the study of intracellular penetration by different types of array of CNFs still requires further investigation and will not be discussed here.

Many aspects of the VACNF synthesis by catalytically controlled plasma enhanced chemical vapour deposition (PECVD), and direct current PECVD in particular, have been extensively studied (Ren *et al* 1998, Chhowalla *et al* 2001, Merkulov *et al* 2002a). To grow VACNFs, a catalyst metal (e.g. Ni) is first deposited on a substrate at predefined locations. This substrate is placed onto the cathode of a glow discharge system and heated to approximately 700 °C in a flow of acetylene and ammonia. After the plasma is formed, CNFs grow from the defined catalyst dots. According to the model developed by Baker (1989), carbonaceous species decompose at the surface of and diffuse through the catalyst particle and are incorporated into a growing nanostructure between the particle and the substrate. Such nanofibres, with the catalyst particle at the tip, grow oriented along the electric field lines of the dc-PECVD (Merkulov *et al* 2002b). The diameter of the nanofibres coincides with the size of the catalytic particle. Their length can be precisely controlled by the growth time, which in case of PECVD is completely determined by the time the plasma is on. That is, the growth can be interrupted by turning off the high voltage of the plasma discharge and then can be reinitiated by turning the voltage back on. Additionally, it is possible to change the shape of the CNFs as they can be made more conical or more cylindrical depending on growth conditions, particularly gas composition (Merkulov *et al* 2001b).

Even with this high degree of control, there are limitations to the controlled growth of isolated individual VACNFs, based on previously reported methods. In particular, in sparse arrays of VACNFs, the catalyst particle reduces in size during growth and ultimately is entirely etched away (Merkulov *et al* 2001b). Thus, the ultimate nanofibre length that can be achieved is limited by the total amount of catalyst available, and the sputtering rate of this particle during growth. Another issue in using existing methods is that, in order to produce a *single* isolated nanofibre at each location, the initial catalyst dot diameter must be approximately 100 nm or smaller (Merkulov *et al* 2000). This size requirement limits the amount of catalyst available for fibre growth, and therefore constrains the ultimate length of fibres that may be achieved. Further, definition of $<$100 nm diameter dots is not easily achievable in a cost effective manner and requires expensive lithography tools that are often unavailable to the research community (e.g. electron beam lithography (EBL)). Overcoming these limitations is crucial for many potential applications. Even though there have been reports of methods to produce sparse stochastic and ordered arrays of VACNFs on a large scale (Huang *et al* 2003, Tu *et al* 2003), these methods do not provide such control over the location and size of catalyst nanoparticles as is offered by lithographic techniques.

In this paper we present a method for preparation of sparse arrays of individual, high-aspect-ratio, long (5–20 μm), conical, VACNFs on a large scale (whole wafers). The catalyst particle preparation method is based on the following factors:

(a) utilization of photolithography as an inexpensive and scalable means to define sparse arrays;
(b) control of the geometry of the initial patterned catalyst dot, i.e., its thickness-to-diameter ratio determines the number of catalyst nanoparticles produced per dot;
(c) pre-growth treatment of the catalyst dots in order to nucleate single particles during the initial stage of CNF growth.

The rigidity of the resultant VACNFs was achieved by selecting an appropriate range of growth parameters at which the Si substrate is etched and redeposited on the sidewalls of the CNFs.

2. Experimental details

Arrays of 500 nm diameter circular dots were photolithographically defined on a 5 cm $\times$ 5 cm area in a square grid pattern at 5 μm intervals on 100 mm diameter n-type silicon wafers (photoresist OiR 620-7i, exposed by GCA AutoStep200). After electron-gun physical vapour deposition of 10 nm of a Ti buffer layer and 200 nm of Ni, metal lift-off by dissolution of photoresist in acetone resulted in definition of catalyst discs (called 'dots' throughout this paper) as shown in figure 1. VACNF growth was then accomplished using PECVD. The wafer was maintained at a temperature of 700 °C, while a mixture of acetylene and ammonia was introduced into a PECVD chamber at 3 Torr total pressure. The plasma was initiated and maintained at 450 V and 300 mA. Growth of individual fibres resulted from catalytic deposition of carbon, which diffuses through the nickel particle at the growing-fibre tip, and also by non-catalytic deposition of material on the fibre sidewalls. The synthesized VACNFs were analysed using a Hitachi S-4700 scanning electron microscope (SEM) equipped with two secondary electron detectors. Due to the geometry of their placement, by combining the signal of these two detectors, images that show compositional detail of the nanofibres beyond the surface morphology can be produced. Hence, this technique was used to image the shape and position of the catalyst nanoparticle within the CNF without resorting to the use of a transmission electron microscope that would require removal of the CNFs from the substrate and placement onto imaging grids. The SEM was also equipped with an x-ray energy dispersive spectroscopy (EDS) detector (Oxford Instruments 7200) and used in 'Point&ID' mode to determine the elemental composition of fibres with spatial resolution. For transmission electron microscopy (TEM) imaging using a Phillips 100 kV microscope, the nanofibres were scraped off the substrate and suspended in water. The suspension was then spotted and dried onto a Cu grid with lacy carbon.

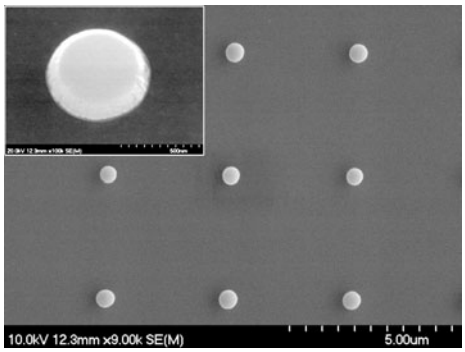

Figure 1. Scanning electron micrograph of an array of Ni dots 500 nm in diameter ($d = 500$ nm), 200 nm in height ($h = 200$ nm) and 5 μm apart. Inset: a magnified view of an individual Ni dot.

3. Results and discussion

Typical growth resulted in conically shaped fibres of 6–20 μm length (depending upon growth time) with tip diameters of 20–50 nm and base diameters of 500–600 nm. The SEM images of the resultant 12 μm VACNFs are presented in figure 2. These images were obtained in the mode in which secondary electrons are collected in wide range of energies and thus include not only surface but also subsurface signal. This allows distinguishing the bright Ni particle at the tip of each fibre and a cylindrical section right below the particle that appears slightly darker than the remaining conical lower part of the fibre. The TEM images displayed in figure 3 further clarify this structure. Here, the conically shaped catalyst (Ni) particle is located at the tip of a 'herring-bone' structured cylindrical CNF. The CNF is coated by a sheath of amorphous material that is visible in the lower part in figure 3(a). The elemental composition of this material depends on C_2H_2/NH_3 gas flow ratio during growth. This dependence has been previously described in Merkulov *et al* (2002a). It has been reported that the sidewall sheath consists of a mixture of C, N and O. By comparing EDX spectra (figures 4 and 5) from VACNFs on Si substrate and on TEM grids (not containing Si) we found that Si is another major component of this material (figure 5(b)), thus the sheath around CNFs is composed of Si, N and possibly some C. The influence of the substrate on plasma composition during PECVD growth of CNFs so far has been disregarded in modelling (Hash *et al* 2003, Meyyappan *et al* 2003) but in fact should be taken into account. Such deposits occur only at low C_2H_2/NH_3 ratios. At higher ratios, the substrate is protected by amorphous carbon film that is continuously formed and etched away. At these high ratios, the nanofibre is composed of pure carbon. Such carbon film can be accumulated on the sidewalls and lead to conically shaped fibres as was reported before (Merkulov *et al* 2001a). At even higher C_2H_2/NH_3 ratios, thick carbon film covers the whole surface and prevents growth (Melechko *et al* 2002).

For these fibres, the quantitative analysis of atomic composition determined by EDX at different points on the fibre both on the Si substrate and the TEM grid (lacy carbon on Cu, on Al sample holder) is summarized in table 1. From this analysis we can conclude that the core of the structure is a CNF with no doping, with a Ni particle at its tip and a Si–N–C containing sheath deposited on the sidewalls of the nanofibre. To further confirm this observation we have used reactive ion etching in SF_6-based plasma to remove the sheath. SF_6-based recipes are usually used to etch Si or silicon nitride and do not significantly affect carbonaceous materials (e.g. photoresist). As a result of this etching, we have obtained cylindrical nanofibres that contained only carbon according to EDX analysis.

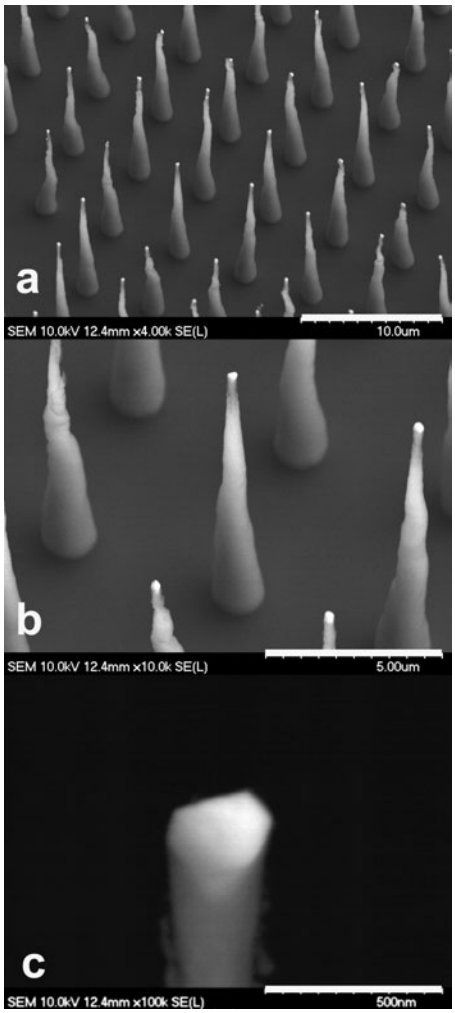

Figure 2. Scanning electron micrograph of an isolated high-aspect-ratio nanofibre and an array of VACNFs at 30° viewing angle. The scale bar is 10, 5 and 0.5 μm in (a), (b) and (c) respectively. The brighter area at the tip of the nanofibre is a Ni catalyst particle.

Two new insights into catalyst preparation allowed us to grow *isolated* single fibres from photolithographically defined catalyst dots. First was the realization that it is the aspect ratio (thickness-to-diameter (h/d figure 1)) of the initial dot, rather than diameter alone as previously reported (Merkulov *et al* 2000), that determines the number of nanofibres which grow from each catalyst dot. Second was the re-evaluation of the pre-growth processing steps that resulted in elimination of a pre-etching step that has been usually used to prepare catalyst particles from contiguous thin film of catalyst. Previously, this pre-etch step has been exposure of the substrate to NH_3 plasma at high temperature (e.g. 700 °C) for about 30–60 s.

It has been reported that the size of the catalyst particles that form by annealing a thin, contiguous film depends on

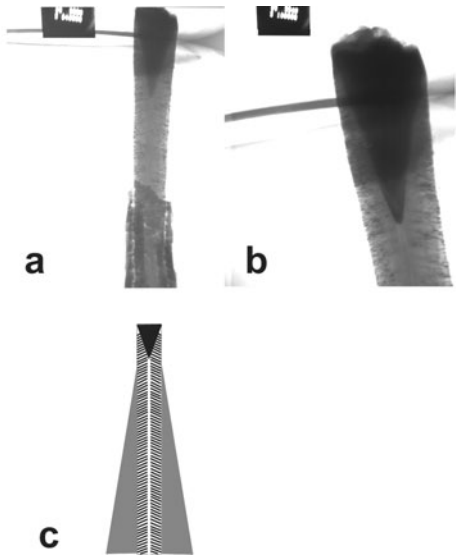

Figure 3. (a), (b) Transmission electron micrographs of VACNFs placed on lacy carbon grids. The darker triangular shaped area at the top is a Ni catalyst particle. The darker area in the lower part of the fibre in (a) is a silicon and nitrogen containing sheath formed during VACNF synthesis. (c) Schematic representation of the structure of the nanofibre that has a triangular shaped catalyst particle at the tip, cylindrical carbon core with a herring-bone type structure and silicon nitride conical sheath deposited on the sidewalls of the CNF core.

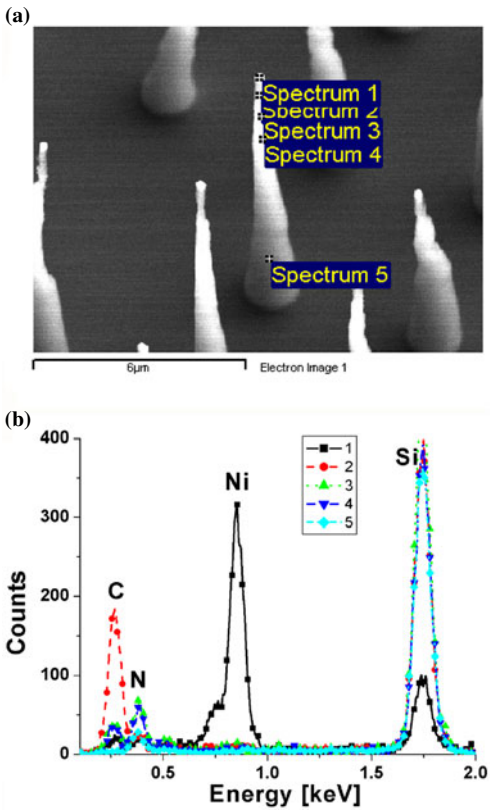

Figure 4. EDX spectra acquired at different points on a VACNF located on Si substrate and tilted at 30° with respect to the electron beam.

the thickness of the film (Chhowalla *et al* 2001), where the number of particles per unit area is smaller for thicker films. We have exploited this property to produce single

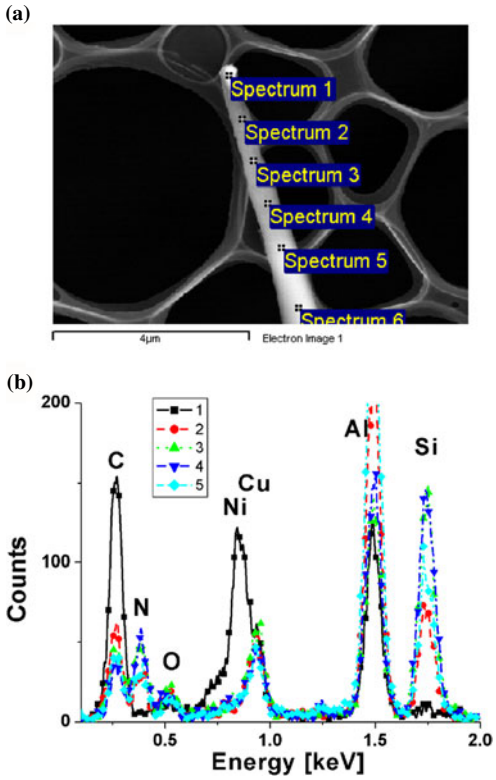

Figure 5. EDX spectra acquired at different points on a VACNF that has been removed from the Si substrate and placed on a lacy carbon grid. The Si peak arises solely from the material that has been sputtered from the Si substrate during VACNF synthesis. The C peak is a combination of signal from the nanofibre and the underlying grid. The Cu and Al peaks arise from the TEM grid and sample holder respectively.

Table 1. (a) Elemental composition determined by EDX in atomic per cent at different locations on the VACNF on the Si substrate (figure 4(a)). (b) Elemental composition determined by EDX in atomic per cent at different locations on the VACNF on a TEM grid (lacy carbon on Cu grid placed on Al sample holder) (figure 5(a)).

		1	2	3	4	5
(a)	C	0.00	81.46	29.00	29.09	0.00
	N	0.00	18.54	45.58	46.91	51.16
	O	0.00	0.00	0.00	0.00	0.00
	Ni	20.40	0.00	0.00	0.00	0.00
	Si	79.60	0.00	25.41	24.00	48.84
(b)	C	73.54	39.92	29.90	27.05	35.65
	N	0.00	28.39	39.88	41.56	35.16
	O	0.00	7.81	7.63	7.85	0.00
	Ni	13.26	0.00	0.00	0.00	0.00
	Si	0.00	5.88	10.28	11.14	8.46
	Cu	4.80	3.55	3.83	2.88	2.68
	Al	8.40	14.45	8.49	9.51	18.08

particles from large diameter dots. The SEM images presented in figure 6 demonstrate the dependence of the number of catalyst nanoparticles formed and therefore the number of CNFs grown, on the thickness of the catalyst dots (10, 40, 80 and 160 nm) with the same diameter (500 nm). The average number of nanoparticles that were formed during the pre-growth processing step decreases with an increase in the height-to-diameter aspect ratio as is illustrated in figure 7.

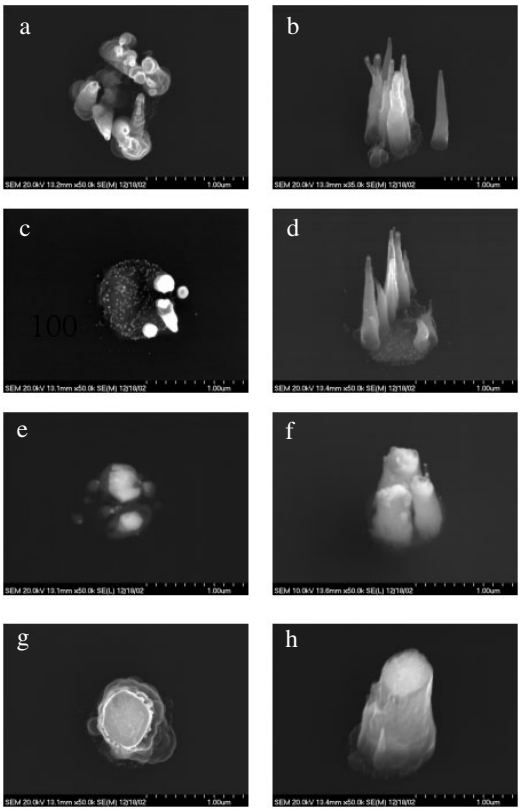

Figure 6. Scanning electron micrographs of VACNFs viewed perpendicular to the substrate (left-hand column) and at 30° tilt from the normal (right-hand column). The left- and right-hand images are acquired from different dots. The initial thickness of Ni prior to growth was (a), (b) 10 nm; (c), (d) 40 nm; (e), (f) 80 nm; (g), (h) 160 nm. The growth time was 5 min. The scale bar is 1 μm.

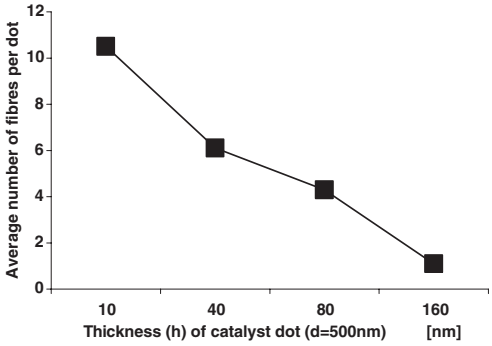

Figure 7. Average number of catalyst particles (and therefore nanofibres) per dot produced from a Ni dot that is 500 nm in diameter versus the initial thickness of Ni on each dot. The averaging was based on ten dots for each thickness.

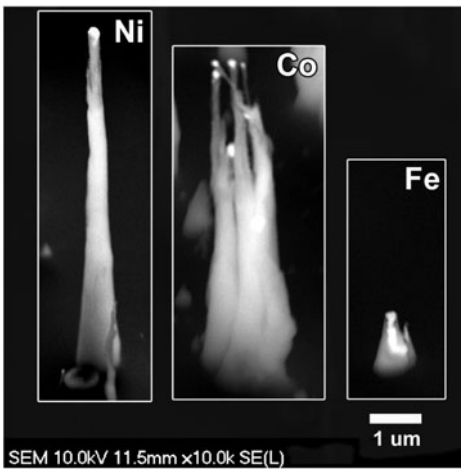

Figure 8. Scanning electron micrographs of high-aspect-ratio nanofibres produced from 200 nm of Ni, Co and Fe 500 nm diameter dots synthesized in a single experiment (growth time 60 min) at 30° viewing angle. The scale bar is 1 μm. The brighter areas at the tips of the nanofibres are Ni, Co and Fe catalyst particles, respectively.

This result is also dependent on the growth conditions, as discussed below. The nanofibres shown in figure 6 were synthesized under identical growth conditions (gas flow, temperature, pressure, plasma current and bias) following an identical process sequence. The growth conditions are important through the first stages of growth, until the catalyst nanoparticles detach from the substrate. In fact, it has been shown that the initial growth conditions determine even whether the particle will stay on the substrate ('base-type' growth mode) or will be lifted off it by the growing nanofibre ('tip-type' growth mode) (Melechko *et al* 2002).

In order to prepare nanoparticles from a thin continuous film of Ni, the samples are typically subjected to an etch in NH_3 plasma for periods of 30–60 s at 700 °C. As this suggests, the pre-growth etch step facilitates the formation of small catalyst dots from the larger catalyst film, which results in a dense forest of CNFs. However, in order to grow single fibres from large dots, the formation of smaller catalyst dots is not desired, and we have eliminated this step. Instead, we introduce acetylene into the chamber a few seconds prior to initiating the plasma, which facilitates the formation of a graphitic carbon film on the surface of Ni. This thin film protects the catalyst from etch, and the associated fracturing, when the plasma is initiated. Introducing the acetylene too much in advance of plasma initiation leads to either complete encapsulation of the substrate with a thick solid carbon film and no nanofibre growth, or, at lower acetylene/ammonia flow ratio, to growth of base-type nanofibres where the catalyst particles remain attached to the substrate (Melechko *et al* 2002). In this latter case, the growth proceeds as a result of thermal chemical vapour deposition, leading to randomly aligned and poorly controlled nanofibres.

We have also compared growth from Co, Fe and Ni. Figure 8 displays SEM images of CNFs that were synthesized simultaneously and thus under the same conditions. Quadrants of a 100 mm Si wafer were patterned with 500 nm diameter dots in photoresist and coated with 200 nm of Ni, Co and Fe on top of a 10 nm Ti buffer layer. The conditions used for fibre growth were the same as those described above. Ni dots retained their integrity and produced single nanofibres per dot on most of the dots; however, Co dots split into multiple particles and produced multiple fibres on all dots. It is possible that growth from 500 nm diameter Co dots could result in single fibres if the thickness of the metal were increased; however, we were not able to deposit thicker catalyst since the the film and photoresist peels off the substrate during the deposition of films thicker than 200 nm due to stress. Fe dots resulted in single or multiple particles with a very stretched shape with

Fe distributed along almost the whole length of the nanofibre. The growth rate of the fibres with Fe catalyst was considerably smaller than the growth rate of fibres with Ni and Co. From these experiments it appeared that Ni is the best choice for the purpose of producing arrays of isolated, single, conical VACNFs.

In most of our work we used a layer of Ti as a buffer layer to prevent formation of nickel siliside. Thin layers of titanium nitride and silicon dioxide have also been used for this purpose (Teo *et al* 2003). Recently, we have found that the layer of native oxide that forms on the surface of Si in air is a sufficiently good buffer layer. Due to different wetting properties, Ni dots (500 nm in diameter) as thin as 100 nm deposited directly on such oxidized Si surfaces produced single nanofibres on each dot.

4. Conclusions

We have demonstrated deterministic growth of arrays of long (up to at least 20 μm), high-aspect-ratio, spatially isolated, rigid VACNFs from photolithographically defined dots. Such structures are required for many applications including parallel gene delivery into mammalian cells, electrochemical probes and scanning probe tips. This new degree of controlled synthesis of VACNFs adds to previously described methods to control location, diameter, length, orientation, shape and chemical composition. Furthermore, we have demonstrated the key role of the catalyst treatment during the earliest stages of growth. Yet, a complete understanding of the complex behaviour of the catalyst material during the initial stages VACNF growth requires further investigation. For example, it is believed that the catalyst particle has a faceted shape during growth and thus it is a crystalline solid (Toebes *et al* 2002). This assumption is corroborated by the fact that the temperatures used during synthesis are much lower than the melting temperature of the material (Ni). However, the nanoparticle must be liquid at some point in time because it changes its shape during the initial growth stage from a flat disc to a more ball-like or even rodlike geometry. The role of different interfaces, such as catalyst–substrate and thin films at the surface of the catalyst, such as 'native' oxides, adsorbates and carbon films formed during growth, requires further investigation. We have also shown that the substrate material can be an important component of the plasma in the PECVD process and can be utilized for lateral reinforcement of CNFs by sidewall redeposition during their growth.

Acknowledgments

The authors wish to thank P H Fleming for assistance with metal depositions. This work was supported in part by the National Institute for Biomedical Imaging and Bioengineering under assignment 1-R01EB000433-01 and through the Laboratory Directed Research and Development funding programme of the Oak Ridge National Laboratory, which is managed for the US Department of Energy by UT-Battelle, LLC, and in part at the Cornell Nanofabrication Facility (a member of the National Nanofabrication Users Network) which is supported by the National Science Foundation under grant ECS-9731293, its users, Cornell University and Industrial Affiliates.

References

Baker R T K 1989 Catalytic growth of carbon filaments *Carbon* **27** 315–23

Chhowalla M, Teo K B K, Ducati C, Rupesinghe N L, Amaratunga G A J, Ferrari A C, Roy D, Robertson J and Milne W I 2001 Growth process conditions of vertically aligned carbon nanotubes using plasma enhanced chemical vapour deposition *J. Appl. Phys.* **90** 5308–17

Guillorn M A, McKnight T E, Melechko A, Merkulov V I, Britt P F, Austin D W, Lowndes D H and Simpson M L 2002a Individually addressable vertically aligned carbon nanofiber-based electrochemical probes *J. Appl. Phys.* **91** 3824–8

Guillorn M A, Melechko A V, Merkulov V I, Hensley D K, Simpson M L and Lowndes D H 2002b Self-aligned gated field emission devices using single carbon nanofiber cathodes *Appl. Phys. Lett.* **81** 3660–2

Hash D, Bose D, Govindan T R and Meyyappan M 2003 Simulation of the dc plasma in carbon nanotube growth *J. Appl. Phys.* **93** 6284–90

Huang Z P, Carnahan D L, Rybczynski J, Giersig M, Sennett M, Wang D Z, Wen J G, Kempa K and Ren Z F 2003 Growth of large periodic arrays of carbon nanotubes *Appl. Phys. Lett.* **82** 460–2

Hudspeth Q M, Nagle K P, Zhao Y P, Karabacak T, Nguyen C V, Meyyappan M, Wang G C and Lu T M 2002 How does a multiwalled carbon nanotube atomic force microscopy probe affect the determination of surface roughness statistics? *Surf. Sci.* **515** 453–61

Iijima S 1991 Helical microtubules of graphitic carbon *Nature* **354** 56–8

Lee C J, Lee T J and Park J 2001 Carbon nanofibres grown on sodalime glass at 500 °C using thermal chemical vapour deposition *Chem. Phys. Lett.* **340** 413–8

Li J, Cassell A, Delzeit L, Han J and Meyyappan M 2002 Novel three-dimensional electrodes: electrochemical properties of carbon nanotube ensembles *J. Phys. Chem.* B **106** 9299–305

Matthews K, Cruden B A, Chen B, Meyyappan M and Delzeit L 2002 Plasma-enhanced chemical vapour deposition of multiwalled carbon nanofibres *J. Nanosci. Nanotechnol.* **2** 475–80

McKnight T E, Melechko A V, Griffin G D, Guillorn M A, Merkulov V I, Serna F, Hensley D K, Doktycz M J, Lowndes D H and Simpson M L 2003 Intracellular integration of synthetic nanostructures with viable cells for controlled biochemical manipulation *Nanotechnology* **14** 551–6

Melechko A V, Merkulov V I, Lowndes D H, Guillorn M A and Simpson M L 2002 Transition between base and tip carbon nanofiber growth modes *Chem. Phys. Lett.* **356** 527–33

Merkulov V I, Guillorn M A, Lowndes D H, Simpson M L and Voelkl E 2001a Shaping carbon nanostructures by controlling the synthesis process *Appl. Phys. Lett.* **79** 1178–80

Merkulov V I, Hensley D K, Melechko A V, Guillorn M A, Lowndes D H and Simpson M L 2002a Control mechanisms for the growth of isolated vertically aligned carbon nanofibers *J. Phys. Chem.* B **106** 10570–7

Merkulov V I, Lowndes D H, Wei Y Y, Eres G and Voelkl E 2000 Patterned growth of individual and multiple vertically aligned carbon nanofibres *Appl. Phys. Lett.* **76** 3555–7

Merkulov V I, Melechko A V, Guillorn M A, Lowndes D H and Simpson M L 2001b Sharpening of carbon nanocone tips during plasma-enhanced chemical vapour growth *Chem. Phys. Lett.* **350** 381–5

Merkulov V I, Melechko A V, Guillorn M A, Simpson M L, Lowndes D H, Whealton J H and Raridon R J 2002b Controlled alignment of carbon nanofibres in a large-scale synthesis process *Appl. Phys. Lett.* **80** 4816–8

Meyyappan M, Delzeit L, Cassell A and Hash D 2003 Carbon nanotube growth by PECVD: a review *Plasma Sources Sci. Technol.* **12** 205–16

Nolan P E, Lynch D C and Cutler A H 1998 Carbon deposition and hydrocarbon formation on group VIII metal catalysts *J. Phys. Chem.* B **102** 4165–75

Ren Z F, Huang Z P, Wang D Z, Wen J G, Xu J W, Wang J H, Calvet L E, Chen J, Klemic J F and Reed M A 1999 Growth of a single freestanding multiwall carbon nanotube on each nanonickel dot *Appl. Phys. Lett.* **75** 1086–8

Ren Z F, Huang Z P, Xu J W, Wang J H, Bush P, Siegal M P and Provencio P N 1998 Synthesis of large arrays of well-aligned carbon nanotubes on glass *Science* **282** 1105–7

Teo K B K *et al* 2003 Plasma enhanced chemical vapour deposition carbon nanotubes/nanofibres—how uniform do they grow? *Nanotechnology* **14** 204–11

Toebes M L, Bitter J H, van Dillen A J and de Jong K P 2002 Impact of the structure and reactivity of nickel particles on the catalytic growth of carbon nanofibers *Catal. Today* **76** 33–42

Tu Y, Lin Y H and Ren Z F 2003 Nanoelectrode arrays based on low site density aligned carbon nanotubes *Nano Lett.* **3** 107–9